Optics Letters

Monolithic highly efficient 272 W nested-ring structured-core thulium fiber laser at 1940 nm

RICHARD ŠVEJKAR,^{1,*} MARTIN P. BUCKTHORPE,¹ BÁRA ŠVEJKAROVÁ,^{2,3} PETER C. SHARDLOW,¹ AND W. ANDREW CLARKSON¹

- ¹Optoelectronics Research Centre, University of Southampton, University Rd., Southampton SO17 1BJ, UK
- ²Institute of Photonics and Electronics of the Czech Academy of Sciences, Chaberská 57, 182 51 Prague, Czech Republic

Received 23 April 2025; revised 23 June 2025; accepted 25 June 2025; posted 30 June 2025; published 4 September 2025

A novel, to the best of our knowledge, thulium-doped silica fiber with a non-uniform core doping profile has been utilized to demonstrate a high-power monolithic laser oscillator system. The fiber laser achieved a continuous-wave (CW) output power of 272W at 1940nm with slope efficiencies of 68% and 71% with respect to launched and absorbed pump power, respectively. This novel Tm fiber design enabled the generation of the highest reported output power from a single-mode, small core (<15 um diameter) non-pedestal fiber. Moreover, the slope efficiency achieved is the maximum reported to date for a single-mode thulium fiber laser operating at >100 W output power level. Published by Optica Publishing Group under the terms of the Creative Commons Attribution 4.0 License. Further distribution of this work must maintain attribution to the author(s) and the published article's title, journal citation, and DOI.

https://doi.org/10.1364/OL.566019

The 2-µm wavelength band is important for various application areas. Over recent years, Tm-doped fiber lasers have emerged as a key player in applications such as medical treatments, materials processing, spectroscopy, remote sensing, non-linear frequency conversion to the mid-infrared band, LIDAR, and various defense applications [1,2]. This has driven the necessity to scale the available output power from these devices, as well as optimizing their efficiency [1,3].

Tm-doped active fibers have the option to be core or cladding pumped. Core pumping typically utilizes a wavelength of 1.55 μm from Er-doped systems, which allow access to shorter lasing wavelengths in Tm^{3+} doped silica emission band [4,5]. However, the power scaling potential is limited due to the difficulties associated with the power scaling of the Er-fiber laser pump source. Cladding pumping by laser diodes at 1710 nm allows direct pumping of upper laser level 3F_4 ; hence, low quantum defect and high laser efficiency can be achieved [6]. However, this method of pumping is not suitable for power scaling because of the immaturity of the diode pump sources, which so far have low brightness and a maximum output power of 80 W. On the other hand, cladding pumping with 790 nm laser diode sources offers significant power scaling potential. For this rea-

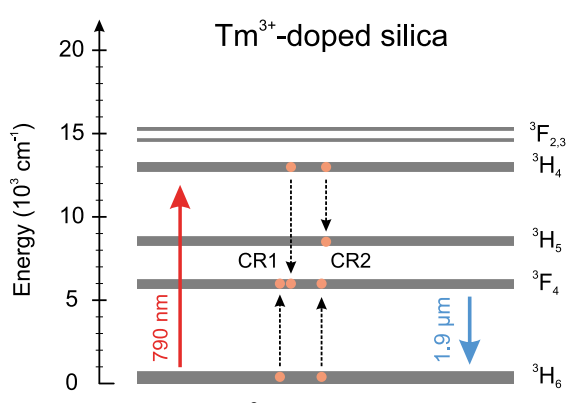


Fig. 1. Energy levels of Tm³⁺ in silica host. CR, cross-relaxation, modified from [1].

son, high-power Tm-doped fiber lasers are generally based on a 790-nm cladding pumping scheme. Through the well-known two-for-one cross-relaxation process, it is possible to achieve up to two signal (laser) photons for each pump photon absorbed, as shown in Fig. 1. This allows the theoretical maximum quantum efficiency of 2 [1,7]. For given pump and laser signal wavelengths of 790 nm and 1940 nm, respectively, the theoretical maximum slope efficiency is 81%. This requires a high doping level of $Tm^{3+} > 3.5 \text{ wt.}\%$), which leads to effective energy exchange between neighboring ions for efficient exploitation of the cross-relaxation process Tm^{3+} ($^3H_4, ^3H_6 \rightarrow ^3\bar{F}_4, ^3F_4$) [8]. This process has allowed demonstrations of cladding-pumped single-mode Tm-fiber lasers in the multi-hundred-watt to kilowatt level in simple oscillator [7,9,10] and master-oscillator power-amplifier (MOPA) configurations [3,11,12]. However, when operating in this output power regime, slope efficiencies are typically below 60% and hence well below the theoretical limit (around 80%) expected when efficiently exploiting the "two-for-one" cross-relaxation process. Indeed, the highest power so far reported for a single-mode all-fiber monolithic cavity oscillator is 680W with a slope efficiency with respect to absorbed power of 44% [13].

In this Letter, we present a Tm-doped fiber laser utilizing a structured (nested-ring) core design delivering a single-mode

³ Faculty of Nuclear Sciences and Physical Engineering, Czech Technical University in Prague, Břehová 7, 115 19 Prague 1, Czech Republic *richard.sveikar@soton.ac.uk

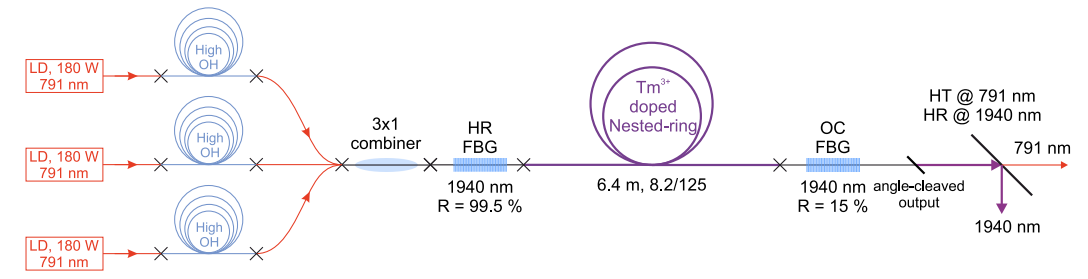


Fig. 2. Monolithic Tm-doped fiber laser setup. HR FBG, high reflectivity fiber Bragg grating; OC FBG, output coupler fiber Bragg grating.

output power of 272 W at 1940 nm with a corresponding slope efficiency with respect to absorbed power of 71%. To the best of our knowledge, this represents the highest efficiency reported for a Tm-doped fiber laser cladding-pumped at 791 nm operating at >100 W output power.

A simple monolithic all-fiber laser configuration was employed, as shown in Fig. 2, with feedback for lasing provided by a high reflectivity (R > 99.5\% @ 1940 \pm 3 nm, bandwidth $1.5 \,\mathrm{nm}$ at $-3 \,\mathrm{dB}$) fiber Bragg grating (FBG) spliced to the pump input end of the active Tm fiber and an output coupler FBG with reflectivity R = 15% @ 1940 ± 3 nm and bandwidth 0.42 nm at -3 dB spliced to the output end of the active fiber. The active fiber was fabricated in house with a non-uniform (ring-shaped) Tm doping profile, which we refer to as a nested-ring design. The confinement of Tm³⁺ doping to a thin ring towards the outer edge of the fiber core reduces the spatial overlap between the propagating fundamental mode and the doped region reducing the gain for parasitic emission at longer wavelengths in the Tm emission band compared to conventional uniformly doped double-clad Tm fibers facilitating efficient operation at mid-band wavelengths (1907 nm for example [2]). The spatial overlap is fairly uniform across the wavelength band of interest but is lower than in standard uniformly doped fibers, leading to reduced gain at all wavelengths. This helps suppress parasitic emission at longer wavelengths, though in our nested-ring fiber the effect is marginal, with the main benefit being reduced thermal loading density. One of the main advantages of this design is also reducing the pump absorption per unit length and hence thermal loading density, while still maintaining a high Tm³⁺ doping concentration within the doped region of the core (4 wt.%), to enable efficient exploitation of the "two-for-one" cross-relaxation process. Thermally induced degradation or damage to the fiber's polymer outer coating is typically the main limiting factor on average output power for conventional double-clad Tm fiber designs, so this design feature offers the potential for considerably higher output power to be achieved before the thermal limits are reached [2]. The nested ring active fiber used in our experiments is shown in Fig. 3 and has the following specifications: concentration of Tm3+ 4 wt.%, core diameter 8.2 µm (NA=0.15), and an octagonshaped silica inner cladding with dimensions 122 µm (flat-toflat) and 132 µm (corner-to-corner) with cladding NA 0.46. The robustness of the single-mode operation was simulated using Optiwave OptiFiber software to confirm that only supported mode is fundamental LP₀₁. Complete fiber specifications and more details about this type of nested-ring fiber can be found in [2].

Pump light at 791 nm was provided by three 180W fiber-coupled laser diodes supplied by AeroDiode with $105/125\,\mu m$ (0.22 NA, $2\,\mu m$ signal isolation of 30 dB) delivery fibers that

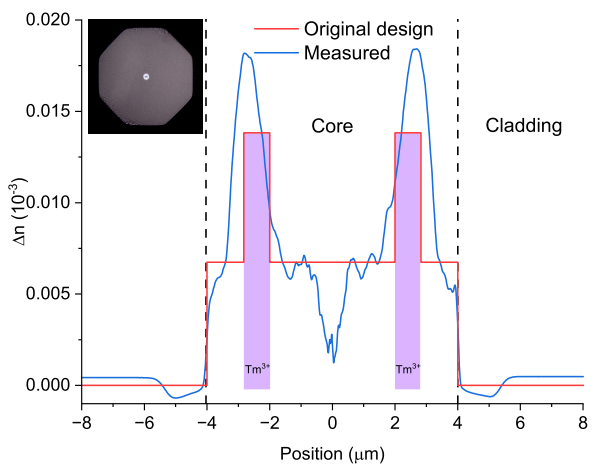


Fig. 3. Refractive index profile of Tm-doped nested-ring fiber with Tm³⁺ confinement, top left inset is photography of fiber from microscope.

were spatially combined with the aid of a tapered fiber bundle (Gooch & Housego, TFB-MMM312A81, 3×1 , output fiber $10/125\,\mu m$, NA 0.15/0.45). The pump power per diode was limited to $164\,W$ to minimize any power degradation, resulting in a maximum of $492\,W$ of pump available. This was further reduced by the tapered fiber bundle transmission loss and splice losses to yield a maximum pump power of $460\,W$ launched into the Tm fiber.

A superluminescent diode (SLED, 790 \pm 40 nm) source was used to measure transmission in a short piece (6.4 cm) of active fiber to evaluate the absorption spectrum presented in Fig. 4. The absorption spectrum ($^3H_6 \rightarrow ^3H_4$) has its maximum value at 787 nm; therefore, the diode pump wavelength during the laser experiments was temperature tuned to 790 \pm 1 nm to be close to this maximum. The effective pump absorption coefficient for pump light launched into the fiber's inner cladding was determined via a cut-back measurement to be 2.1 dBm $^{-1}$ corresponding to an overall absorption efficiency of 95% for the 6.4-m length of active fiber in use.

As a precaution against possible damage to the pump diodes from parasitic lasing at longer wavelengths in the Tm emission band 12-m coils of high OH fiber (Thorlabs, $105/125\,\mu m$, $0.22\,NA$) were spliced between each diode and the pump combiner. The latter has high absorption in the two-micron band preventing any parasitic emission from reaching the diodes. Finally, the output pigtail of the OC FBG was angle cleaved (8°) to prevent broadband feedback to the oscillator and thereby help prevent parasitic lasing. Residual pump power was separated from the Tm fiber laser output in free-space by a dichroic mir-

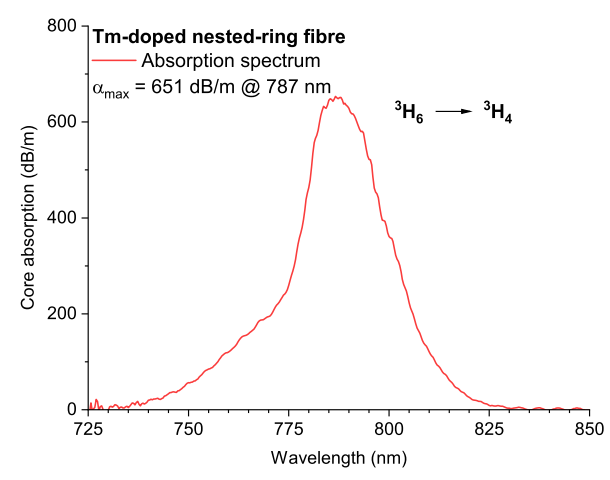


Fig. 4. Absorption spectrum of nested-ring Tm-doped fiber.

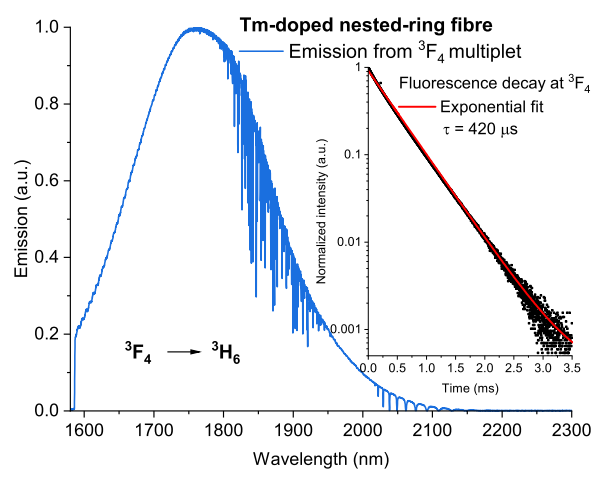


Fig. 5. Emission spectrum of nested-ring Tm-doped fiber, inset lifetime measurement at ${}^{3}F_{4}$ multiplet.

ror with a transmission of 94.5% @ 791 and reflectivity of 98.65% @ 1940 nm. All fibers and laser components were actively cooled using water-cooled heat sinks maintained at 17°C to provide effective thermal management. Tight bending was avoided to prevent signal leakage into the polymer coating. The output power at 1.94 μ m and unabsorbed power at 791 nm were measured by Gentec-EO PS-1K and UP19K-110F-H9 power meters, respectively, both with a power calibration uncertainty $\pm 2.5\%$. Laser emission wavelengths were measured using an optical spectral analyzer (OSA) Yokogawa AQ6375 (resolution 0.05 nm). The laser beam spatial profile was measured for an attenuated collimated beam by the Spiricon Pyrocam IIIHR (pixel size 75 μ m, active area 12.8 \times 12.8 mm). All splices were performed using a Fujikura FSM-60S arc fusion splicer.

Prior to operating the laser, preliminary experiments were performed using an in-house built Er-fiber laser emitting at 1565 nm as a pump source to measure the emission spectrum (${}^3F_4 \rightarrow {}^3H_6$) of the Tm-doped nested ring active fiber, as presented in Fig. 5. It can be observed that the measurement reveals a number of narrow absorption lines from 1800 nm to 1950 nm due to water vapor in the free-space part of the diagnostic arrangement. Ideally, the Tm fiber laser's operating wavelength should be fine-tuned to avoid these and hence any loss of out-

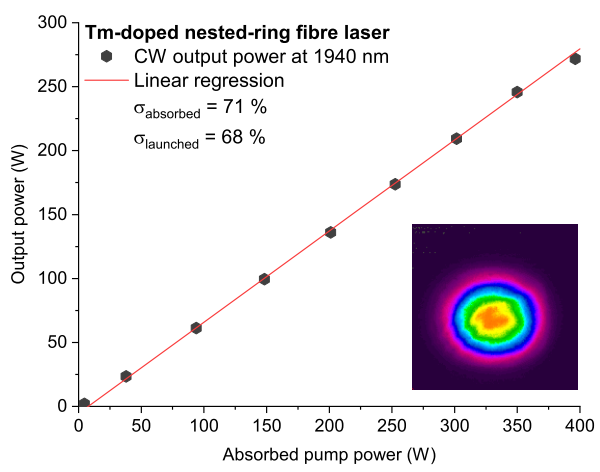


Fig. 6. Output laser characteristics for CW laser operation, bottom right inset—beam profile at 100W; $\sigma_{absorbed}$ and $\sigma_{launched}$ —slope efficiencies for absorbed and launched pump power.

put power. The inset in Fig. 5 shows the fluorescence decay time for upper laser level 3F_4 . The measured data are fitted by a first-order exponential decay curve. From an average of several measurements, the decay time was evaluated to be $420 \pm 6 \mu s$. More details about fluorescent decay, lifetime measurements, and data processing can be found in [14]. Even though the nested-ring active fiber has a structured core, its spectroscopic parameters are comparable with those of commonly used uniformly doped Tm-doped active fibers [1,15,16].

Figure 6 shows the measured output power of the laser system as a function of absorbed pump power, including a correction factor to account for the 3.4% loss at the output angle cleaved facet. The angle of the output facet must be precise, and the facet must be kept clean; otherwise, the output fiber suffers from failure due to laser fusing. During operation, pump power was slowly increased up to 414W of incident power (396W absorbed power). The inset of Fig. 6 shows the output beam transverse intensity profile (at 100 W), indicating that this is dominated by the LP₀₁ fundamental mode. The M² value for multi-watt level operation was determined to be 1.06 for both x- and y-axes as expected since the output beam emerges from a single-mode passive fiber that only supports the LP₀₁ mode. However, due to significant heating of the collimating aspherical lens (f = 14.8 mm, AR coated at 2 µm) at power levels exceeding 100 W and residual water vapor absorption causing thermal blooming there is some degradation in the output beam at high power levels resulting from the free-space diagnostic setup. No methods to resolve this issue (e.g., using a dry nitrogen atmosphere) were practical in our setup. For this reason, a determination of the M² parameter was limited to low powers to confirm the single-mode nature of the output fiber. The maximum output power of 272 W was achieved at an absorbed pump power of 396 W. This represents the highest output power in the two-micron band for pedestal-free fibers up to a core diameter of 15 μ m. This corresponds to slope efficiencies of 71 \pm 2% and $68 \pm 2\%$ with respect to absorbed and launched pump power, respectively, and, to the best of our knowledge, represents the highest published efficiency for powers exceeding 50 W. The upper limit on output power in our experiment was determined by the onset of damage to the splice between the passive and active

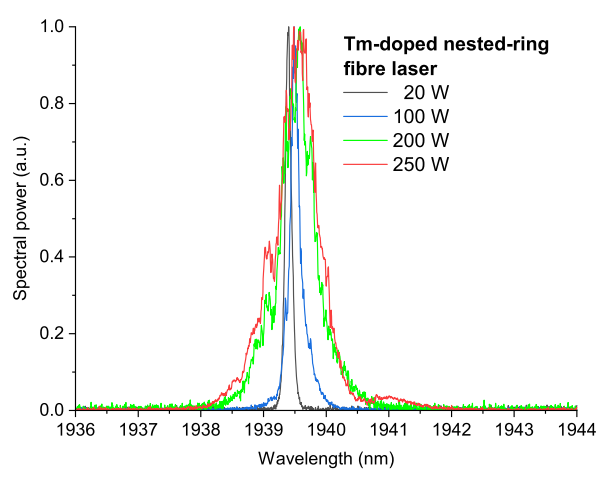


Fig. 7. Recorded optical spectra of emission lines at various output power levels.

fiber at the pump input end of the oscillator. This is believed to be due to a small amount of pump light leaking from the splice due to a slight mismatch in the circular passive and octagonal active inner claddings. Further optimization of the active Tm fiber to allow a slightly larger inner cladding size would be expected to remedy this problem, allowing further power scaling. It is worth noting that the theoretical efficiency of 81.5%, derived from the quantum defect and assuming a 100% efficient 2-for-1 process, represents an upper limit. In high-power systems, the observed quantum efficiency is closer to 1.85 [17], which brings the practical limit down to about 76%. Additionally, background propagation losses at $2\,\mu m$ further attenuate the signal and should be considered [18].

The results presented in Fig. 7 show the laser emission spectra recorded by Yokogawa AQ6375 spectrum analyzer at different output power levels up to 250 W. Before discussing the results it is important to note that both HR and OC FBGs have technical specifications, as previously stated, that were guaranteed up to 200W of pump and 100W of signal power. The laser was operated significantly above these values. Even though the FBGs were actively water cooled to 17°C, one can see that the full-width-half-maximum (FWHM) emission line broadens from 0.12 nm at 20 W output up to 0.59 nm at 250 W output. Up to 170 W of output power, the linewidth correlates with the specification of the OC FBG. It is also evident that there is a small shift in the central emission wavelength towards longer wavelengths as the power is increased. The latter observations are consistent with heating of the FBGs due to residual absorption at the lasing wavelength resulting in chirping of the FBG period.

In conclusion, we have presented a high-power monolithic "all-fiber" laser system utilizing a novel nested-ring Tm active fiber. The maximum output power achieved was 272 W at 1940 nm and with a corresponding slope efficiency of $71\pm2\%$ with respect to absorbed pump. Compared to previous publications [2], we increased the output power almost five times and managed to increase efficiency while maintaining purely single-mode operation, which, we believe, is a significant improvement and progress in $2\,\mu\text{m}$ laser research. This non-uniform core design has allowed effective power scaling and fundamental mode emission from a small core design without the use of a pedestal

layer. To the best of our knowledge, this result represents the highest slope efficiency for a Tm fiber laser operating in the multi-hundred-watt regime. In our experiments, the upper limit on output power was determined by the onset of damage to the splice between the pump input passive fiber and the active Tm fiber. Even so, these results are believed to be close to the thermal damage limit of the active fiber's polymer outer coating. Further modification to the fiber design (e.g., using a thinner Tm-doped ring) to spread heat loading over a longer length of fiber should offer the potential to scale to significantly higher power, benefiting a range of applications.

Funding. Engineering and Physical Sciences Research Council (EP/W028786/1); Ministerstvo Školství, Mládeže a Tělovýchovy (LasApp CZ.02.01.01/00/22_008/0004573).

Acknowledgment. The authors would like to thank Petr Vařák, Ph.D. for his help with fluorescence decay time measurement.

Disclosures. The authors declare no conflicts of interest.

Data availability. Data underlying the results presented in this paper are available online at Ref. [19].

REFERENCES

- A. Sincore, J. D. Bradford, J. Cook, et al., IEEE J. Sel. Top. Quantum Electron. 24, 1 (2018).
- M. J. Barber, P. C. Shardlow, P. Barua, et al., Opt. Lett. 45, 5542 (2020).
- M. Michalska, P. Honzatko, P. Grzes, et al., J. Lightwave Technol. 42, 339 (2024).
- M. D. Burns, P. C. Shardlow, and W. A. Clarkson, in 2021 CLEO/Europe-EQEC (2021), p. 1.
- J. Pokorný, J. Aubrecht, B. Jiříčková, et al., in Specialty Optical Fibres (International Society for Optics and Photonics, 2023), Vol. 12573, paper 125730L.
- J. Šulc, M. Němec, J. Kratochvíl, et al., in Fiber Lasers XXI: Technology and Systems (International Society for Optics and Photonics, 2024), Vol. 12865, paper 128651A.
- T. Walbaum, M. Heinzig, T. Schreiber, et al., Opt. Lett. 41, 2632 (2016)
- P. F. Moulton, G. A. Rines, E. V. Slobodtchikov, et al., IEEE J. Sel. Top. Quantum Electron. 15, 85 (2009).
- B. R. Johnson, D. Creeden, J. Limongelli, et al., in Fiber Lasers XIII: Technology, Systems, and Applications (International Society for Optics and Photonics, 2016), Vol. 9728, paper 972810.
- C. Louot, A. Motard, T. Ibach, et al., IEEE Photonics Technol. Lett. 35, 553 (2023).
- 11. C. Ren, Y. Shen, Y. Zheng, et al., Opt. Express 31, 22733 (2023).
- C. Romano, D. Panitzek, D. Lorenz, et al., J. Lightwave Technol. 42, 394 (2024).
- C. Louot, F. Sanson, A. Motard, et al., in Fiber Lasers XXII: Technology and Systems (International Society for Optics and Photonics, 2025), Vol. 13342, paper 133420P.
- 14. P. Vařák, I. Kašík, P. Peterka, et al., Opt. Express 30, 10050 (2022).
- 15. S. D. Agger and J. H. Povlsen, Opt. Express 14, 50 (2006).
- M. Kamrádek, J. Aubrecht, P. Vařák, et al., Opt. Mater. Express 11, 1805 (2021).
- M. Grábner, B. Švejkarová, J. Aubrecht, et al., J. Lightwave Technol. 42, 2938 (2024).
- M. D. Burns, P. C. Shardlow, P. Barua, et al., Opt. Lett. 44, 5230 (2019)
- R. Svejkar, "Data in support of the 'Monolithic highly-efficient 272 W nested-ring structured-core thulium fibre laser at 1940 nm," University of Southampton, 2025, http://eprints.soton.ac.uk/id/eprint/502712.